Coolability of a Corium Pool in a Debris Bed -Impact of Debris Size, Steam and Liquid Flowrate, Tilting Angle and Pressure on Critical Heat Flux (CHF)

C. Sartoris, T. Garcin, F. Fichot

Coolability of a Corium Pool in a Debris Bed – Impact of Debris Size, Steam and Liquid Flowrate, Tilting Angle and Pressure on Critical Heat Flux (CHF)

Sartoris C., Garcin T., and Fichot F.
Institut de Radioprotection et de Sureté Nucléaire
Cadarache, 13115, BP3, Saint Paul lez Durance
christine.sartoris@irsn.fr; thierry.garcin@irsn.fr; florian.fichot@irsn.fr

ABSTRACT

In case of severe accident in a light water reactor, a debris bed may form in the core and possibly melt, as it happened in TMI-2. Knowledge about the coolability of such molten pool surrounded by debris is crucial to investigate the possibility of stabilizing a part of the fuel inside the vessel. In particular, it is of primary interest to determine the maximum size of a molten pool surrounded by debris which may be stabilized under water.
The maximum heat flux (CHF) that may be extracted from the pool boundary by water flowing within the debris bed is a key parameter. A facility was built at IRSN to determine the CHF under various conditions. A heated copper surface simulates the boundary of the pool and is placed in contact with a debris bed (monodisperse steel balls), under water.
In this article, we first complete previous work on steam flowrate impact and we show the slight impact of liquid flowrate. We then illustrate the influence of the ball diameter and we compare to the situation of pool-boiling without any debris near the heated plate. All those tests are made for different tilting angles of the plate. In a last part, we study the impact of pressure with an extra pressure level of 1.5 bar abs.
As a conclusion of this work and of results previously published, a general CHF correlation depending on the tilting angle and the steam flowrate is derived. An example of the use of this correlation to evaluate the maximum mass of corium pool that can be stabilized under water is given, for some typical reactor conditions.

KEYWORDS
Severe accident, Corium coolability, Critical Heat Flux, Pool-boiling, Debris bed

1. INTRODUCTION

In case of a severe accident in a nuclear reactor, a large debris bed may be created in the core. If, in some part of this debris bed, the temperature keeps on rising up to the melting point, it may form a molten pool of corium, as it happened in TMI-2 (Broughton [1]). The molten pool is expected to become less and less coolable as it grows larger because the heat flux at the periphery of the pool increases linearly with the pool diameter. Therefore, it is of primary interest to determine the maximum size of a molten pool surrounded by debris which may be stabilized under water after reflooding the vessel (as in TMI-2) or in case of a debris bed formed in a flooded reactor pit where the presence of denser zones may limit the coolability (Kudinov et al.[2], Hwang et al. [3]). The maximum heat flux that may be extracted, or Critical Heat Flux (CHF), is a key parameter for that issue.

In pool boiling, tilting angle impact on CHF has been studied extensively in literature. In 1999, Howard and Mudawar [4] made a review gathering quasi-static or quenching tests, carried out with different fluids

(water, liquid helium, freon, ethanol, R113, FC-72,…), saturated or under-saturated, for different surface materials (copper, platin, stainless steel, aluminium,…), of different dimensions and shapes, and for different tilting angles. Among these studies, only Guo and El Genk [5] present CHF for a copper surface in deionized water for different tilting angles. But these are quenching tests. Mei and al. [6] and Tanjung and Jo [7] present quasi-static tests with deionized water, copper surface and several tilting angles. Their results are represented in the following when compared with our own results in paragraph 5.3. Jeong's [8] and Yang and al.'s [9] works have also been considered for comparison, despite the stainless steel surface.
The open literature related to CHF along a heated plate immersed in a debris bed is much more limited than the one concerning CHF along a heated plate in a water pool. Sartoris and al. [10] briefly present these works. Fukusako and al. [11], Spencer [12] and Tung and Dhir [13] studied different boiling regimes for different surface materials, shapes and orientations, and different ball materials and sizes. Fukusako and Tung and Dhir showed that CHF increases with ball diameter. Fukusako gave correlations for a few boiling curve characteristics. Spencer correlated the CHF with the elevation along a vertical heated plate and observed surface aging phenomenon. Wang and Beckermann [14] derived a model for the dry-out heat flux.
In none of these works are the effect of surface orientation or the effect of steam or liquid flowrate investigated. Gong and al. [15] studied the effect of key parameters on CHF: tilting angle, fluid mass flux and inlet quality. In their tests, dry-out occurs on a stainless steel surface in contact with deionized water in a rectangular channel. They show that CHF increases with the increase of water mass flux (from 110 to 288 kg/m2.s), quality (from 0.003 to 0.036), and decreases when tilting angle increases from 90° to 165° (according to our angle convention).

Sakashita [16] studied the CHF dependency on pressure. He and some other authors he cites showed that CHF behavior with pressure agrees quite well for liquids other than water. For water, the conclusions differ with the exchange surface shape or size. Most of Kazakova tests mentioned in Sakashita, conducted on wire and ribbon surfaces of different sizes, agree with Zuber or Lienhard and Dhir correlations, derived from Kutateladze correlation. But Sakashita and Ono tests – carried out with an upward facing surface – and Kasakova's ones - carried out with a 0.29 mm wire – provide higher CHF values. Sakashita completed these CHF data by conducting tests with a vertical 7 mm copper surface and different fluids and in particular with water from 1 to 8 bar abs. In this case, he shows that CHF cannot be reached over the whole range of pressures by fitting the Kutatelatze correlation with coefficient K as usual. Sakashita shows that this difference can be reduced by accounting for water wettability change with pressure thanks to the dependency with temperature of the contact angle between the steam bubbles and the surface.

The present work is the continuation of former work related in [10]. The corium pool (a section of the pool actually) is simulated by a copper plate which can be tilted to describe different sections of the corium pool (see Fig. 1). A deionized water tank filled with steel balls simulates the flooded debris bed. The CHF values are measured for 2 mm and 4 mm ball diameters. The choice of debris size was made according to observations made in the core debris formed during TMI-2 accident (Broughton [1]), and according to more fundamental considerations about fragmentation of fuel pellets (Coindreau and al. [17). Previous experiments performed in this former work [10] allowed us to study the effect on CHF of tilting angle from 90° to 150°, with and without upwards steam flowrate. The present experiments complete the steam flowrate investigation with pure deionized water (no balls) in pool-boiling conditions for angles from 90° to 150°. For these most inclined angles, the effect of upcoming liquid flowrate has also been evaluated with and without balls. Moreover, this work broadens the tilting angle range down to 0° (horizontal upward surface) for 2 mm and 4 mm diameter balls and with deionized water only. Eventually, the pressure effect on CHF is evaluated at 1.5 bar abs.

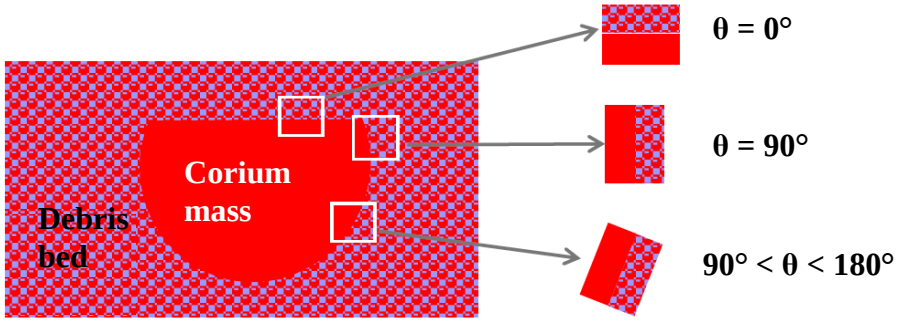

Figure 1. Description of the Contact Surface between Corium Mass and Debris Bed.

2. EXPERIMENTAL APPARATUS

The objective of the experiments is to measure the CHF on a flat surface in contact with a monodisperse steel ball bed or with pure deionized water. In all the tests, water is at a temperature near saturation. For atmospheric conditions experiments, the experimental apparatus is described in [10] and recalled here. The 50 mm diameter copper electrically heated surface (heated plate) is in contact with a bed filled with 2 mm or 4 mm steel balls and deionized water or only deionized water (see Vertical Plate ("VP") test section drawing in Fig. 2 (left). Experiments involving liquid or steam flowrate are performed in the Steam Generator "SG" test section illustrated on Fig. 2 (right). This last section enables steam generation by electrically heating a copper block situated below the 50 mm cylinder previously described. A mono-diameter bed filling is privileged, unlike former experiments where bigger balls were placed in front of the steam generator to postpone its dry-out. These two test sections may be tilted from 90° (vertical heated plate) to 150° downward.

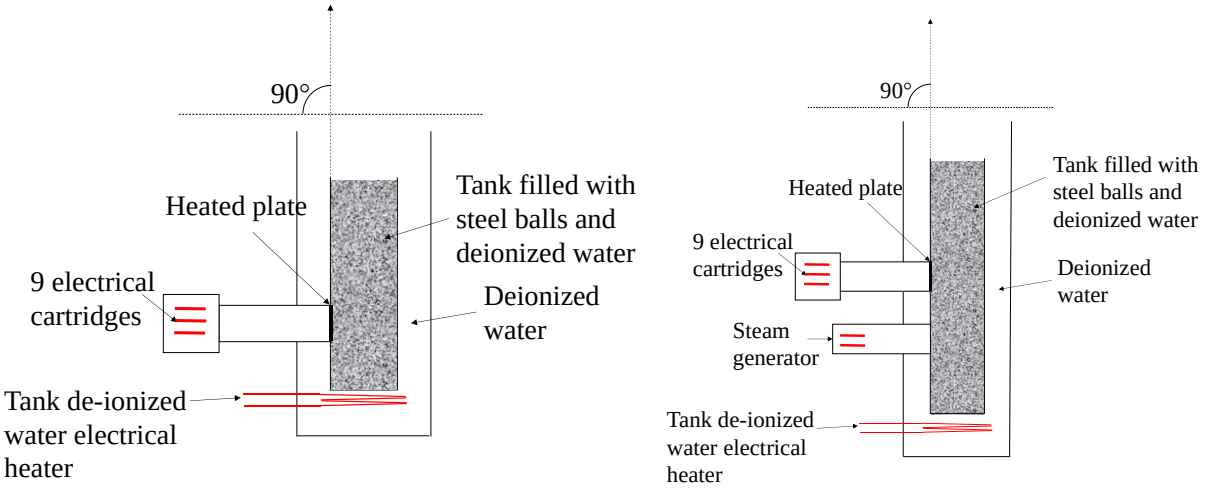

Figure 2. Schematic of the "VP" Test Section (left) and "SG" Test Section (right)

Additionally, for experiments involving near horizontal tilting angles, the Horizontal Plate "HP" test section is used (Fig. 3). This test section does not enable any steam or liquid flowrate. It can be tilted from 0° to 30°.

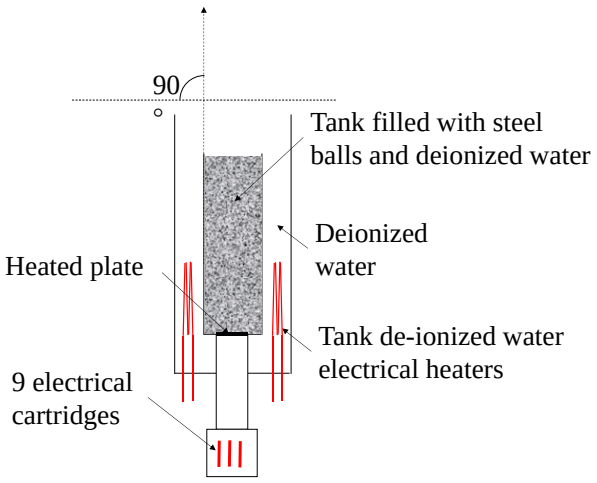

Figure 3. Schematic of the "HP" Test Section

All the external surfaces are thermally insulated.

For the tests involving liquid flowrate, "SG" test section is connected to a loop allowing saturated water injection at section and debris bed bottom (Fig. 4).

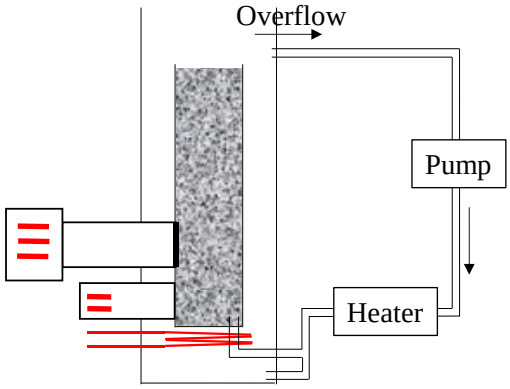

Figure 4. Schematic of the "SG" Test Section Connected to Liquid Loop

For pressurized tests, "SG" test section (Fig. 5) has been strengthened and adapted to be connected to a water tank situated above. This tank level imposes the pressure in the test section due to the water column weight. A cooler has been placed at test section exit to avoid flashing in the water column.

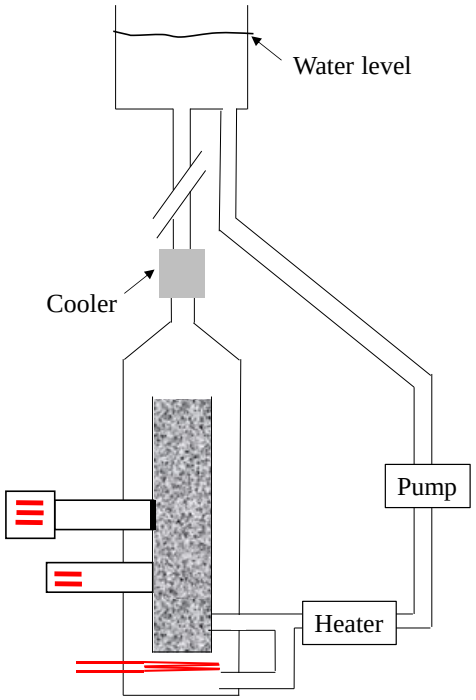

Figure 5. Schematic of the Pressure Test Section

3. INSTRUMENTATION, MEASURE, HEAT FLUX CALCULATION AND UNCERTAINTIES

The heated cylinder is equipped with at least twelve 1 mm-diameter type K thermocouples, positioned along the four azimuths. They are used to estimate the heat flux transferred to the debris bed (see Fig. 6).

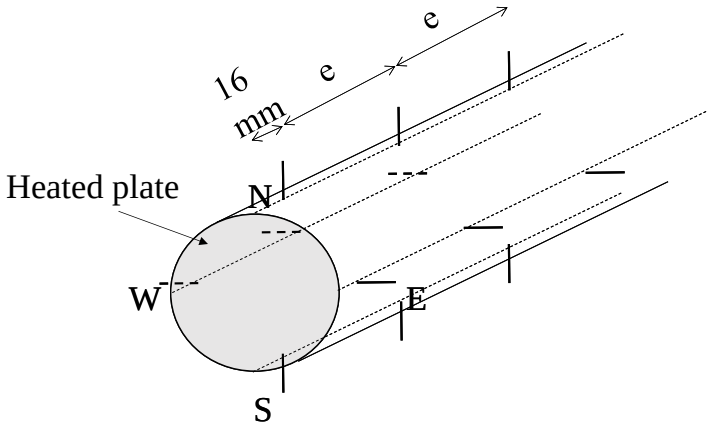

Figure 6. Implantation of the Twelve Thermocouples inside the Heated Cylinder.

This heated cylinder length may differ from a sample to another. Some of them are said “long” ones and the distance between their thermocouples is 100 mm. In the “short” ones, their thermocouples are implanted at only 10 mm from one another. Some of these short ones have been designed or adapted to be used with an actuator moving the heating cartridges block back just after the CHF achievement. Indeed, in

some of the most energetic cases, the section leaktightness may be threatened, the gasket placed between the heated plate and the section being overheated.
Other type K thermocouples and PT100 sensors are positioned in the balls bed at about a few centimeters in front of the heated plate and in the channel to check the water saturation.

A flowmeter is used for tests with liquid flowrate and for pressurized tests, a pressure sensor is connected to the test section at the heated surface level.

For each azimuth, the heat flux is derived from the temperature measurement of the two extreme thermocouples by Fourier's law:

$$\Phi = \frac{\lambda}{e}.(T_1 - T_2) \quad (1)$$

with λ being the copper thermal conductivity ($W.m^{-1}.K^{-1}$), *e* the distance between the thermocouples providing the temperatures T_1 and T_2 (K).
The value of the heat flux varies with the azimuth. In the following, the heat flux values correspond to the east-west averaged value.

The flux relative uncertainty is calculated by error propagation method, thanks to equation (2):

$$\frac{U_{\bar{\varphi}}}{\bar{\varphi}} = \boldsymbol{k}\sqrt{\left(\frac{U_\lambda}{\lambda}\right)^2 + \mathbf{2}.\left(\frac{U_T}{\Delta T}\right)^2 + \left(\frac{U_{\Delta z}}{\Delta z}\right)^2} \quad (2)$$

Where k = 2 for a 95% confidence level.
Thermal conductivity uncertainty and thermocouple distance uncertainty are respectively 10% and 0.8 mm. The uncertainty on temperature measurement is 1.45 °C, including sensors and acquisition system. As we consider uniform absolute uncertainties distributions for all the parameters, these uncertainties must be divided by √3.

4. SURFACE PREPARATION AND HEATING PROCEDURE

The surface preparation and the heating procedure are the same as the ones described in [10]. The surface roughness is lower than 0.3 µm. After heating of the deionized water, a stabilization time is necessary for structures heating and water degassing. Liquid flowrate in the bed is adjusted for tests with convection, steam generator electrical power is set to generate the targeted steam flowrate if needed.
For pressure tests, water is slowly injected in the external water tank in order to push residual steam out of the test section and avoid cooler steam blockage. This injection has no effect on the liquid flowrate in the heated surface vicinity. This water is injected with a few degrees below saturation, and saturation is achieved with the water tank heaters.
The heated surface power, starting from steady-state conditions, is slowly increased (0.09 W/s) to ensure quasi-static conditions. The CHF is considered achieved when the copper mass temperatures dramatically increase. All the heating devices are stopped and the actuator – if used – is recoiled.

5. RESULTS

5.1. Steam Flowrate Impact

Sartoris and al. [10] mention steam flowrate impact for 2 mm - and 4 mm-ball beds for different tilting angles. The case of pure water completes these results. In order to show the steam flowrate impact, the ratio CHF with steam flowrate to CHF without steam flowrate is expressed on Fig. 7.
When the bed is filled with balls, the steam presence tends to decrease the CHF value, particularly dramatically for the smaller balls. An explanation may be that the presence of balls prevents steam from escaping from the heated surface and facilitates a vapor film formation, especially for the 2 mm balls whose small size enables enhanced steam retention due to capillarity phenomenon. On the contrary, without balls, the steam flowrate makes the CHF value slightly increase. This may be induced by enhanced local convection of water by steam bubbles. That convection is of course prevented when balls fill the bed, especially if they are small (high friction factor).

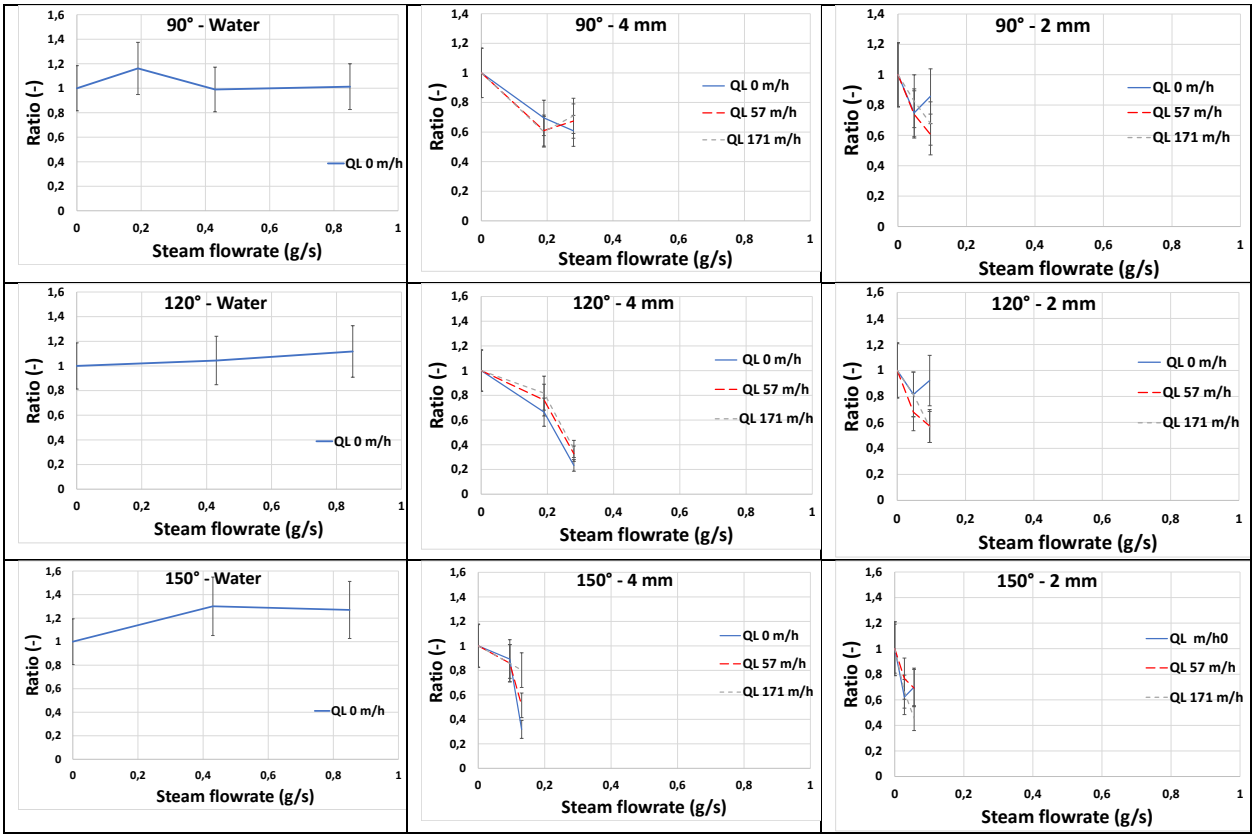

Figure 7. Impact of Steam Flowrate for Different Tilting Angles (rows), for Pure Water, and 4 mm– and 2 mm-Ball Bed.

5.2. Liquid Velocity Impact

Tests with upwards liquid flowrate were performed with pure water and with 4 mm- and 2 mm-ball beds. The maximum imposed liquid flowrate corresponds to a liquid velocity of 60 m/h for pure water and 171

m/h when the bed is filled with balls. In order to show the liquid flowrate impact, the ratio CHF with liquid flowrate to CHF without liquid flowrate is expressed on Fig. 8.
The general tendency is that liquid flowrate slightly enhances CHF value, and the result is about the same for water and balls bed. The only exception case seems to be the most inclined one with the smallest balls where the influence is much more marked. The slight CHF gain due to liquid velocity seems boosted in that case, despite the steam retention close to the surface by the combined effects of strong inclination and capillarity: maybe the dynamic pressure generated by convection is sufficient to overcome the capillary pressure.

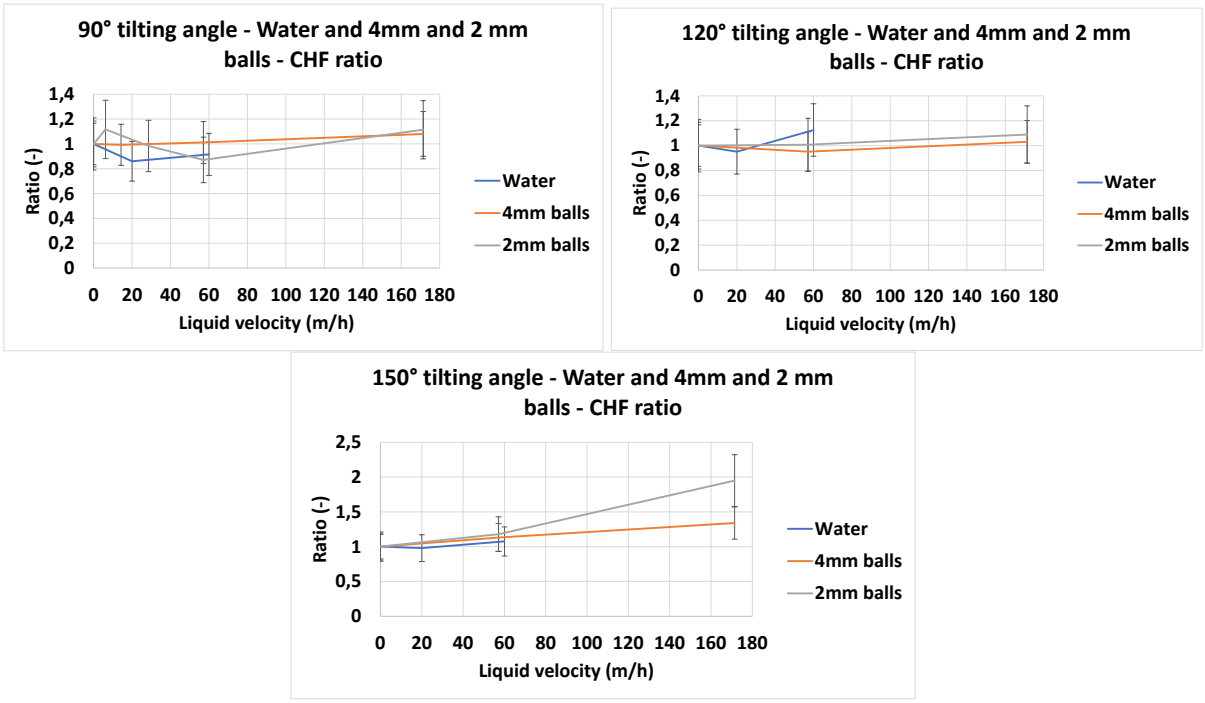

Figure 8. Impact of Liquid Velocity for Different Tilting Angles, for Pure Water, and 4 mm– and 2 mm-Ball Bed.

No comparison with Gong and al.'s results [15] is possible because our maximum liquid mass flux worths about 16 kg/m^2.s^{-1} whereas Gong scanned the range 110 kg/m^2.s -288 kg/m^2.s^{-1}.

5.3 Tilting Angle Impact

For this investigation, the 3 mm intermediate ball diameter has been added. Thus, Fig. 9 (high, left and high, right) gives the CHF results for pure water and 2 mm, 3 mm and 4 mm balls, depending on tilting angle. Thanks to "VP" and "HP" test sections, the whole range of 0°-150° tilting angles was covered. The results obtained in "VP" test section show in full marks, those obtained in "HP" test section in hollow marks. It is noticeable that the CHF values obtained at 30° in "VP" or "HP" test section are different. It is due to the "test section" effect and "heated plate" effects as mentioned in [10]: when performed in different test sections or with different heated plates, the same test conditions lead to different CHF values. No explanation could be found to that phenomenon.
To enable the elaboration of the tilting angle impact on the whole tilting angle range, CHF ratios were estimated with reference to CHF at 30°, which an angle value that is common to both sections. Then it was expressed referring to CHF at 90°, which is a standard reference in literature. Fig. 9 (low, left and

low, right) presents the tilting angle impact on the whole 0°-150° range in term of CHF ratio to 90° CHF, including tests conducted with pure water.

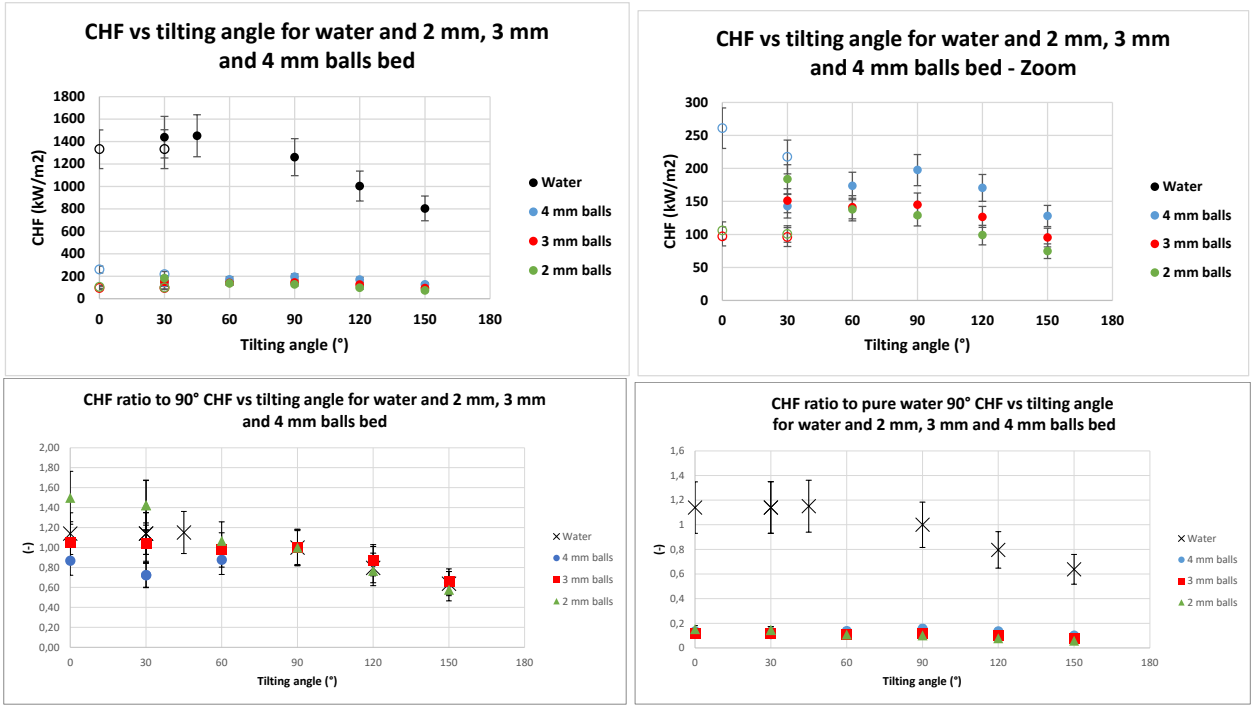

Figure 9. CHF Dependency with Tilting Angle : CHF values (high, left), Zoom (high, right), CHF ratio to 90° CHF (low, left) and CHF ratio to 90° pure water CHF (low, right)

For the tilting angles from 90° to 150°, the tilting angle impact is moderate, and the results are very similar with or without balls. These results confirm those conducted with balls illustrated in [10].
For smaller angles, that is to say when the surface is oriented upwards, the impact is low and the CHF is slightly increased compared to 90° CHF (ratio about 1.15) for water case. For tests conducted with balls, the impact may be considerably higher, either increasing or decreasing, depending on the ball diameter. The smallest balls lead to the highest ratios. This may be explained by capillarity phenomena occurring for such ball diameters and retaining liquid water in contact with the exchange surface.

We compared the results obtained with pure water with results provided in literature [5-9]. On Fig. 10, only the tests performed in [6] and [7] (Mei and Tanjung) are rightfully comparable to ours: they involve the same surface material (copper) and coolant nature (deionized water), a quasi-static power evolution and several tilting angles. They are represented with full lines. The other works, less comparable, appear in dashed lines. For better clarity, a zoom is provided on the right side. The figures show that our results are similar, slightly lower for 120° and 150°. This is satisfying, despite the slightly different surface state of our heated plate. In the literature, the surface is generally new and mirror polished, whereas ours is aged and its roughness is only lower than 0.3 µm (surface ageing is obtained by submitting the surface to repeated dry-outs in order to reach roughly stabilized CHF levels, see [10]). For angles higher than 90°, our results are a bit lower than others but nothing hints that it could be due to the state of the surface.

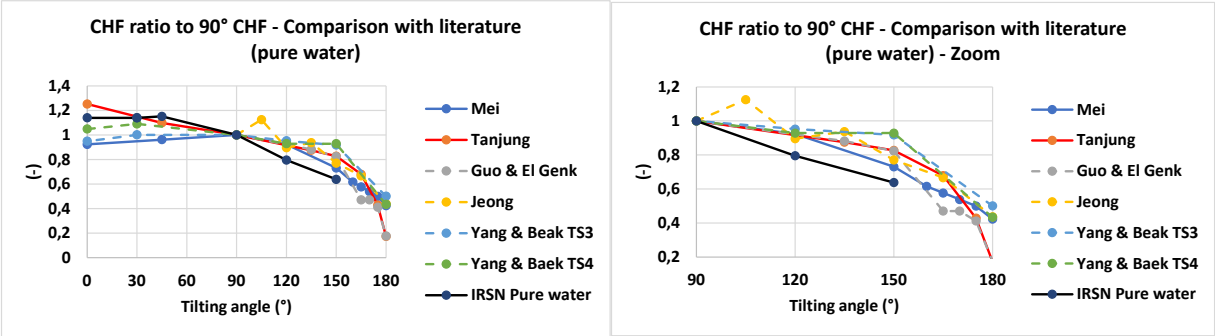

Fig. 10. Comparison of CHF Ratio with Literature – Zoom on the right side

5.4. Pressure Impact

Pressurized tests were conducted in Pressure Test Section positioned so that the surface is placed at 90°. For this angle, our results may be compared with bibliography data.
According to these data, the expected CHF should increase with pressure. Thus, in order to preserve the section gasket leaktightness, pressurized tests have been conducted with 4 mm balls in the bed. Some tests were performed with a liquid flowrate as well, but CHF proved unaffected by it. Thus, all the tests, with and without liquid flowrate, were compiled in Fig. 11.

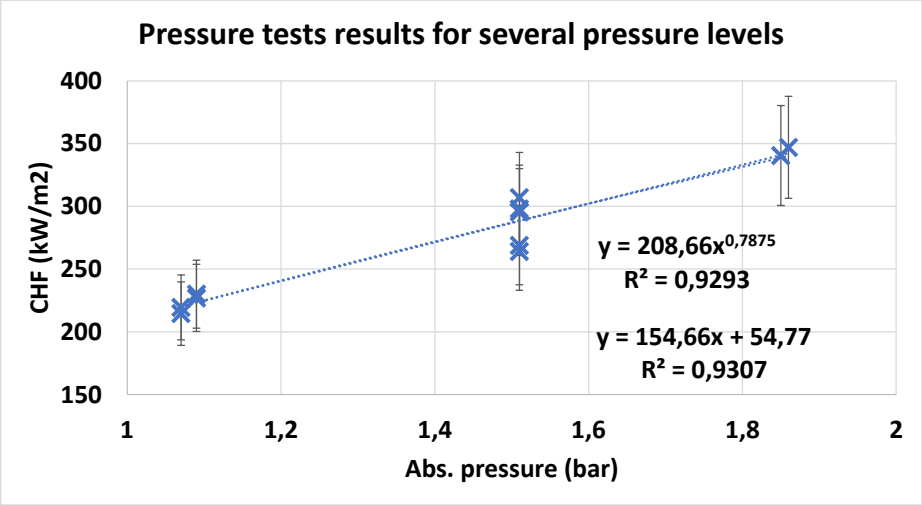

Figure 11. Pressure Tests Results

Fig. 11 shows the CHF values for three pressure levels: about 1.08, 1.51 and 1.85 bar abs. 1.08 bar corresponds to the water level of the filled test section. It is reminded that CHF values relate to an aged surface and would not be comparable to CHF obtained with mirror polished surfaces.
As recalled in Sakashita [16], Kutateladze-type CHF correlation indicates that CHF varies as $\rho_s^{0.5}$, i.e. as $P^{0.5}$. Sakashita (Fig. 10 of [16]) reports CHF data for water higher than Zuber and Lienard and Dhir predictions assuming $P^{0.5}$ dependency. The author explains that this gap is well addressed by taking wettability effects into account. Rough CHF estimation from Sakashita leads to a $P^{0.7}$ dependency for pressures between 1 and 6 bar (see Fig. 12). In our case, the $P^{0.7}$ dependency is in good agreement with the measured data which lead to a dependency in $P^{0.78}$ (see Fig. 11). Our results are then totally consistent with Sakashita ones. A linear dependency shows a slightly better fit but we did not cover a large range of pressure.

These tests may later be completed by higher pressure levels, up to about 2.5 bar abs.

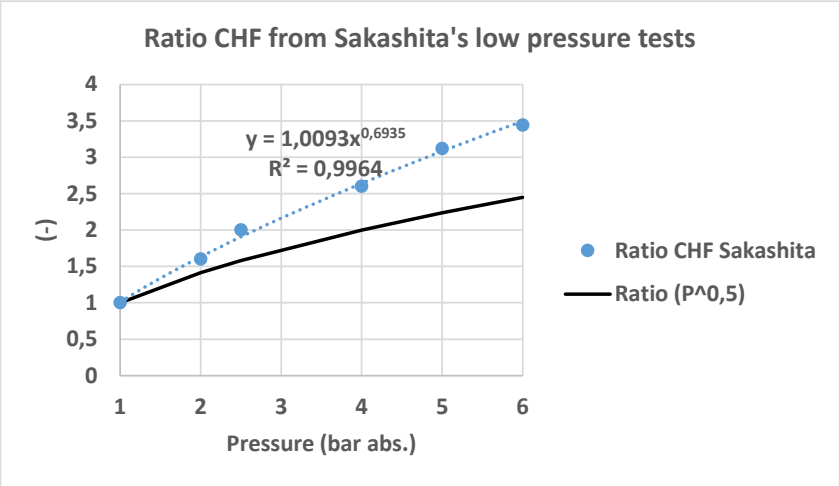

Fig. 12. CHF ratio from Sakashita Pressure Tests with Water [14]

6. EXAMPLE OF A COOLABLE MAXIMUM CORIUM POOL SIZE DETERMINATION WITH CORRELATION DEPENDING ON STEAM FLOWRATE AND TILTING ANGLE

As a result of previous tests, we derived a simple correlation for the downwards-facing orientation (angle between 90° and 180°) and for the 4mm balls [10]:

$$CHF = CHF_{ref}.\max[0;(1-Q_{Steam})].\max[0.5;\sin\theta] \quad (3)$$

The reference value is approximately $CHF_{ref}\sim 200 kW/m^2$ for a tilting angle of 90° (vertical heating plate) and for our "aged" heating plate surface.
With our new data, it is now possible to improve slightly the accuracy of the correlation and add the pressure dependence:

$$CHF = CHF_{ref}.\max[0;(1-Q_{Steam})].\max[0.5;\sin\theta]\left(\frac{P}{P_{ref}}\right)^{0.7} \quad (4)$$

where the reference values are now $CHF_{ref}\sim 220 kW/m^2$ and P_{ref} is atmospheric pressure.
We apply that correlation to a situation where a spherical molten pool of radius *R* is surrounded by a debris bed of porosity 0.4 and debris size 4mm. Although our results are only available up to 2 bar, the correlation is extended to higher pressure (5 bar): this may be partly justified by the similar correlation found by Sakashita [16] up to 6 bar. The corium pool is discretized in a series of layers of thickness *h* and the interface between the molten pool and the debris bed is located at a position (R,θ) or, equivalently (r,z) where r and z are respectively the radius and the elevation of the layer. At each position (or angle) along the molten pool, the local steam flow rate is evaluated by integrating the steam production in the debris bed and along the molten pool in the region located downstream. At the same location, the heat flux coming from the molten pool is estimated by assuming that the total power generated in the corium layer of thickness *h* is transferred to the lateral surface of the layer.
We look for the highest value of R for which the heat flux from the corium pool is lower than the CHF value everywhere along the boundary, which means that the molten pool would be stable due the cooling by water at the periphery. We consider two cases: a volumetric power of 1 MW/m^3 which corresponds approximately to the decay heat of a 1000MWe reactor, 4 hours after scram, and a volumetric power of

0.6 MW/m^3 which corresponds approximately to the decay heat of a 1000MWe reactor, 10 hours after scram. The results are illustrated in Fig. 13 for the volumetric power of 0.6 MW/m^3: we can see that, for *R*=0.63m, the heat flux from the corium pool is lower than the CHF everywhere and that it is almost equal at the top (90° angle). Above this radius, the heat flux from corium exceeds the CHF in the top part of the pool.

For the volumetric power of 1 MW/m^3, at atmospheric pressure, the maximum size of the molten pool is R=0.3m which corresponds to approximately 1 ton of corium. This is a very low value compared to the total mass of corium which is around 100 ton. For a volumetric power of 0.6 MW/m^3, the maximum size of the molten pool is R=0.63m which corresponds to approximately 4 tons of corium. This is also quite small compared to the total inventory. However, the effect of pressure may increase significantly the mass of corium that can be stabilized. This is represented in Fig. 14, where we can see the maximum fraction of total mass that could be stabilized inside the flooded debris bed, as a function of pressure, for the two volumetric power levels. It shows that, for the case of 0.6 MW/m^3, it is possible to stabilize half of the corium mass by flooding the debris bed, if the pressure is around 5bar.

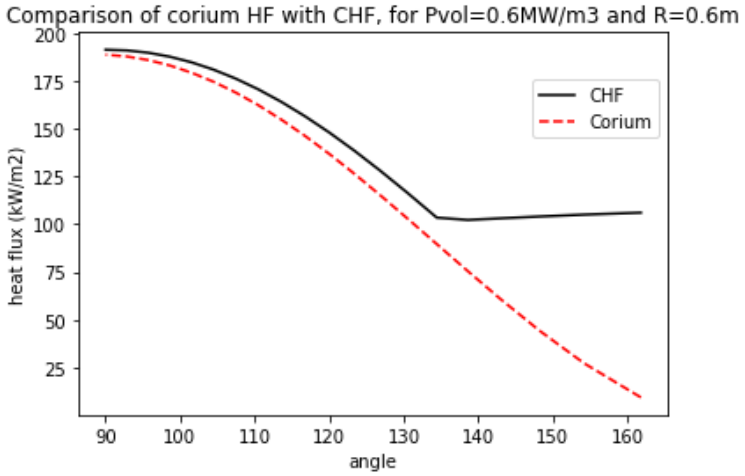

Fig. 13. Comparison of Corium Pool Heat Flux Profile and CHF Profile for Pvol=0.6MW/m3 and R=0.63m

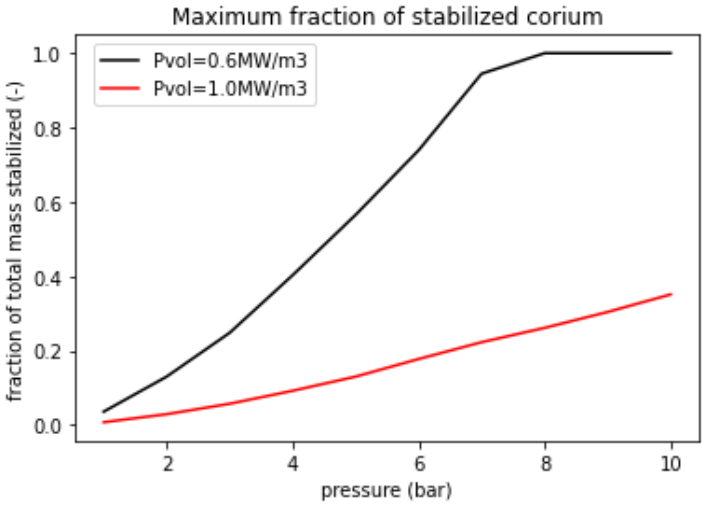

Fig. 14. Maximum fraction of total mass that can be stabilized in a molten pool surrounded by a flooded debris bed

From this simple application study, it can be concluded that, if the pressure is low or the decay heat rather high, once a molten pool has started to grow within a debris bed, it is not possible to stop its progression by reflooding the debris bed. Only very local molten zones can be quenched, the size of such zones being of the order of 30cm to 60cm. On the contrary, if the pressure is around 3-4 bar and the decay heat has decreased, it would be possible to observe the stabilization of a significant amount of molten corium (between 1/3 and ½ of the core inventory) by reflooding the debris bed.

7. CONCLUSION

The experimental apparatus presented in this paper allows to evaluate CHF for a copper surface in contact with a bed made of steel balls and deionized water. Different ball diameters, surface tilting angles, liquid and steam flowrates, and pressure levels were tested.
The present work shows that:

- Tilting angle tends to moderately decrease the CHF in the range 90°-150° in the same extent with or without balls. For smaller tilting angles, CHF is slightly increased, and its variation depends on balls diameter.
- Liquid velocity tends to slightly increase the CHF in our liquid flowrate range,
- For pure water, steam flowrate slightly increases the CHF. On the contrary, it drastically reduces the CHF especially if ball diameter decreases and liquid flowrate rises.
- For pure water, the pressure impact varies closer to $P^{0.7}$ than to $P^{0.5}$ as implied by Kutateladze equation. This is consistent with Sakashita works.
- A correlation has been derived for angles greater than 90°, accounting for pressure, steam flowrate and tilting angle. As an example, this correlation was applied to typical reactor conditions to determine the maximum coolable corium pool size. It was concluded that, at low pressure and shortly after the start of the accident sequence, once a molten pool has started to grow within a debris bed, it is not possible to stop its progression by reflooding the debris bed. Only very local molten zones can be quenched, the size of such zones being of the order of 30cm to 60cm. On the contrary, at higher pressure (in the vessel and the containment) and later in the accident (after half a day), it seems possible to observe the stabilization of almost half of the fuel inventory in a molten pool by reflooding the debris bed surrounding the corium pool.

ACKNOWLEDGMENTS

The authors acknowledge Electricité De France (EDF) for their financial support.

REFERENCES

1. Broughton, J. M., Kuan, P., Petti, D. A., & Tolman, E. L., “A scenario of the Three Mile Island unit 2 accident”, *Nuclear Technology*, **87**, pp. 34–53 (1989) https://doi.org/10.13182/NT89-A27637
2. Kudinov, P., Karbojian, A., Tran, C.T., Villanueva, W. ‘Agglomeration and size distribution of debris in DEFOR-A experiments with Bi2O3-WO3 corium simulant melt’, *Nuclear Engineering and Design*, 263, pp. 284–295. doi: 10.1016/j.nucengdes.2013.06.011.
3. Hwang, B., Moriyama, K., Hwang G., Kaviany, M., Lee, M.,, Kim, E., Park, H.-S., ‘Sensitivity and uncertainty analyses of ex-vessel molten core cooling in a flooded cavity during a severe accident’, *Nuclear Engineering and Design*, 328 (2017), pp. 121–133. doi: 10.1016/j.nucengdes.2017.12.031.
4. A. H. Howard, I. Mudawar, “Orientation effects on Pool Boiling Critical Heat Flux (CHF) and Modeling of CHF for near-vertical Surfaces”, *International Journal of Heat and Mass transfer*, **42**, pp. 1665-1688 (1999)

https://doi.org/10.1016/S0017-9310(98)00233-6
5. Z. Guo, M. El Genk, “An Experimental Study of Saturated Pool Boiling from Downward Facing and Inclined Surfaces”, *International Journal of Heat and Mass transfer*, **35** (9), pp. 2109-2117 (1992). https://doi.org/10.1016/0017-9310(92)90056-X
6. Y. Mei, Y. Shao, S. Gong, Y. Zhu, H. Gu, “Effects of Surface Orientation and Heater Material on Heat Transfer Coefficient and Critical Heat Flux of Nucleate Boiling”, *International Journal of Heat and Mass transfer*, **121**, pp632-640 (2018). https://doi.org/10.1016/j.ijheatmasstransfer.2018.01.020
7. E. Tanjung, D. Jo, “Surface Orientation Effects on Bubble Behaviors and Critical Heat Flux Mechanism in Saturated Water Pool”, *International Journal of Heat and Mass transfer*, **133** pp. 179-191 (2019). https://doi.org/10.1016/j.ijheatmasstransfer.2018.12.113
8. Y. H. Jeong, “Effects of Dimensions and Downward-Facing Angle on CHF under Atmospheric Condition”, *Experimental Thermal and Fluid Science*, **102** pp. 603-610 (2019). https://doi.org/10.1016/j.expthermflusci.2018.10.008
9. S. H. Yang, W-P. Baek, S. H. Chang, “Pool boiling critical heat flux of water on small plates : effects of surface orientation and size”, *International Communications in Heat and Mass Transfer*, **24** (8), pp. 1093-1102 (1997). https://doi.org/10.1016/S0735-1933(97)00103-6
10. C. Sartoris, T. Garcin, F. Fichot, “Coolability of a Corium Pool in a Debris Bed – Critical Heat Flux (CHF) Dependency with Tilting Angle, Debris Size and Steam Flowrate”, *Nuclear Engineering and Design*, **403** (2022) https://doi.org/10.1016/j.nucengdes.2022.112146
11. S. Fukusako, T. Komoriya, N. Seki, “An Experimental Study of Transition and Film Boiling Heat Transfer in Liquid-Saturated Porous Bed,” *Journal of Heat Transfer*, **108**, pp. 117-124 (1986). https://doi.org/10.1115/1.3246875
12. J. Spencer, “Measurement of Critical Heat Flux in a CANDU End Shield Consisting of a Vertical Surface Abutting a Packed Bed of Steel Shielding Balls” *CNL Nuclear Review*, pp. 79-90 (2016). https://doi.org/10.1016/j.net.2021.10.008
13. V. X. Tung, V. K. Dhir, “Experimental Study of Boiling Heat Transfer From a Sphere Embedded in a Liquid-Saturated Porous Medium” *Journal of Heat Transfer*, **112**(3), pp. 736-743 (1990). https://doi.org/10.1115/1.2910448
14. C. Y. Wang, C. Beckermann, “A two-phase mixture model of liquid gas flow and heat transfer in capillary porous media – II: Application to a pressure driven boiling flow adjacent to a vertical heated plate” *Int. J. Heat Mass Transfer*, **36**, pp. 2759-2768 (1993). https://doi.org/10.1016/0017-9310(93)90095-N
15. S. Gong, S. Dong, Y. Mei, B. Zhang, Y. Yuan, Z. Zhang, “Separate Factors’ Effects on CHF for Flow Boiling in an Inclined Rectangular Channel under Low Mass Flux”, *Applied Thermal Engineering*, **207**, 118207 (2022) https://doi.org/10.1016/j.applthermaleng.2022.118207
16. H. Sakashita, “Critical Heat Flux on a Vertical Surface in Saturated Pool Boiling at High Pressures”, *Journal of Thermal Science and Technology*, **11** (2), pp. 1-12 (2016) https://doi.org/10.1299/jtst.2016jtst0020
17. O. Coindreau, F. Fichot, J. Fleurot, « Nuclear fuel rod fragmentation under accidental conditions” *Nuclear Engineering and Design*, **255**, pp. 68–76 (2013) https://doi.org/10.1016/j.nucengdes.2012.09.021